

Derivation of a Reynolds stress response functional for zonal flows from numerical simulations

N. Guertler, K. Hallatschek

Max-Planck-Institut für Plasmaphysik, Garching, Germany

Introduction

Self-consistent numerical studies of ITG-turbulence, using the NLET two fluid code [1], show a Reynolds stress driven zonal flow pattern with a characteristic radial scale length. Based on these observations the requirements for a response functional that can predict the time-evolution and scales of the zonal flows will be analyzed. The long term goal of this research in excitation, damping and time-evolution of zonal flows is to achieve a better understanding of the high-confinement mode and internal transport barriers in fusion devices.

Characteristic scale

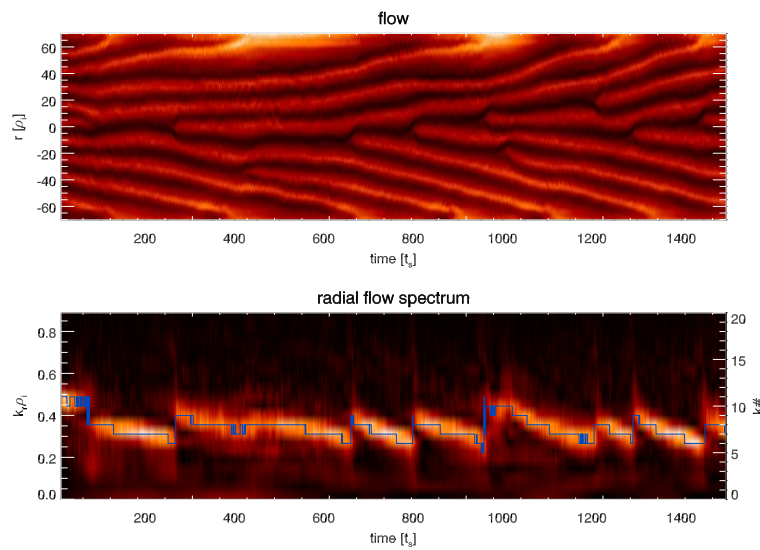


Figure 1: Poloidal zonal flow pattern and radial mode structure. The blue line denotes the dominant k_r and $t_s := 2\pi qR/c_s$. Light/dark color represents a flow in/against the ion-diamagnetic drift direction.

The NLET code was used to simulate the turbulent ITG-system with circular geometry using reduced Braginskii equations with adiabatic electrons described in [1],[2]. The parallel ion heat conductivity was chosen such that temperature perturbations achieve similar damping rates as in kinetic theory. The fluid code is computationally more practical for this analysis than a gyro-kinetic code since a large number of high resolution, long time simulations are required.

Simulations of the core where zonal flows are prevalent show a characteristic flow pattern, fig. 1. The upper figure shows the color coded time-evolution of the flux surface average zonal flow velocity. The flows repel each other and, since the boundary conditions allow them to drift out of the computational domain, the radial spectrum may change slowly over time, lower figure. However, the radial

scale length only varies within tight boundaries as new flows grow to maintain a characteristic scale. Simulations starting from modified initial states with artificial flow patterns always decay into the characteristic zonal flow pattern indicating the robustness of the scale and deterministic flow evolution.

Derivation of a stress response functional

Based on wave-kinetic theory, a response functional for the Reynolds stress R can be constructed, eq. (2), attempting to describe the excitation, saturation and time-evolution of the flux surface average zonal flow velocity \bar{v}_θ using the poloidal force balance, eq. (1) [3]. R contains both the perpendicular and parallel stress components [2]. α, β, γ are constants and I the turbulence intensity, e.g. radial heat transport.

$$\partial_r \bar{v}_\theta = -\partial_r R \quad (1)$$

$$R = I \left[\alpha \partial_r \bar{v}_\theta \left(1 - \beta (\partial_r \bar{v}_\theta)^2 \right) + \gamma \partial_r^3 \bar{v}_\theta \right] \quad (2)$$

For small shearing rates $u := \partial_r \bar{v}_\theta$ only the first term $\alpha \partial_r \bar{v}_\theta$ is relevant and results, inserted in eq. (1), in a zonal flow growth. The non-linear second term becomes more dominant as the shearing rate increases and leads to a flow saturation when $\beta (\partial_r \bar{v}_\theta)^3 \gtrsim \partial_r \bar{v}_\theta$. The third $\gamma \partial_r^3 \bar{v}_\theta$ term models the observed finite width of the flow peaks by damping modes with high k_r . The turbulence intensity I in (2) accounts for the proportionality of the stress and the local turbulence level.

Insertion of a self-consistent time-evolution of a flow pattern into the functional (2) reproduces the associated stress pattern quite well, using appropriate values for α, β and γ . However, the prediction of the observed flow pattern from an initial flow state fails, as a numerical simulation of (1) and (2) always shows the same behavior, fig. 2: Modes with high k_r are quickly damped and flows with low k_r decay into the largest mode that fits into the domain. This is contrary to the turbulence simulations where arbitrary initial flow states always decay into the characteristic zonal flow pattern.

A mean-field theory approximation of $\partial_r (u)^3 \approx 3 \langle u^2 \rangle k_r^2 \bar{v}_\theta$ yields an estimate for the zonal flow growth rate Γ , given by eq. (3). The average is denoted by $\langle \rangle$. The k_r^4 term damps large k_r for all shearing rates u . An increase in the shearing rate u further confines the k_r region with positive growth rate from the high k_r side. When $\beta \langle u^2 \rangle$ approaches $1/3$ only a small region of growing k_r around $k_r = 0$ remains, explaining the decay of the flow pattern into the smallest possible k_r .

$$\Gamma(k_r, u) = I k_r^2 \left(\alpha (1 - 3\beta \langle u^2 \rangle) - \gamma k_r^2 \right) \quad (3)$$

Observations of quick damping of small k_r in self-consistent simulations suggest an extension to

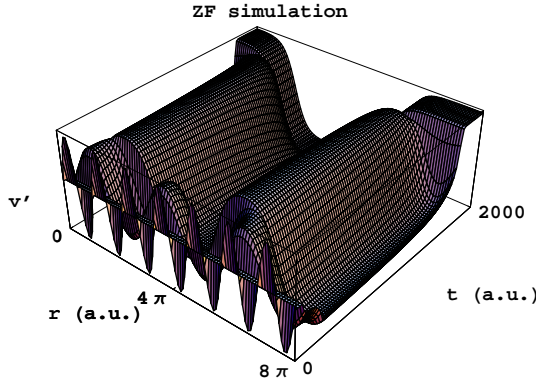


Figure 2: Decaying zonal flow evolution using response functional (2).

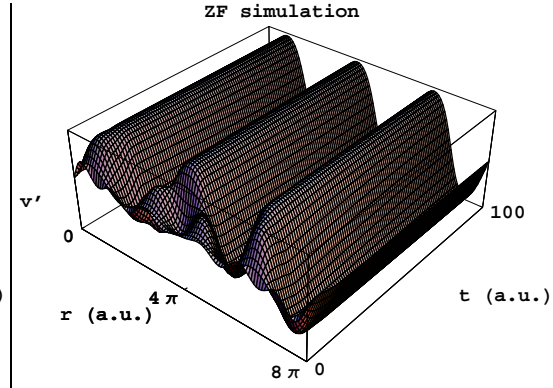


Figure 3: Non-decaying zonal flow evolution using extended functional (5).

the response functional that confines the region with positive growth rate from the small k_r side. A possible behavior for the growth rate that would eliminate the decay into the largest mode is sketched in figure 4. For a non-zero shearing rate u the small k_r modes would be damped before the higher modes. This would leave a localized region of intermediate k_r where flows continue to grow. This region would get more confined until all k_r are damped and the flows saturate at a distinct zonal flow scale.

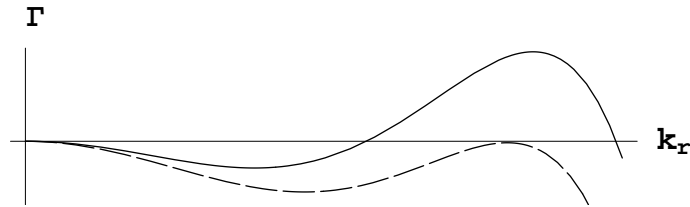


Figure 4: Proposal of zonal flow growth rate Γ with respect to k_r . The dashed line depicts a higher shearing rate u than the continuous line.

constant factor δ .

$$\Gamma(k_r, u) = Ik_r^2 (\alpha(1 - 3\beta \langle u^2 \rangle) + \gamma(k_r^2 - \delta k_r^4)) \quad (4)$$

Translation of this growth rate behavior into a response functional yields equation (5). Numerical solution of (1) with this new stress functional, starting from arbitrary initial states, now results in stationary flow pattern with an characteristic intrinsic scale, fig. 3, depending on γ and δ .

$$R = I \left[\alpha \partial_r \bar{v}_\theta \left(1 - \beta (\partial_r \bar{v}_\theta)^2 \right) - \gamma \left(\partial_r^3 \bar{v}_\theta + \delta \partial_r^5 \bar{v}_\theta \right) \right] \quad (5)$$

One way to obtain this dip for small k_r that respects the symmetry requirements of the fluid equations, is a change of sign in the third term to allow a damping of small k_r through the first and second term while the intermediate k_r still have a positive growth rate. The damping at the high k_r end is handled by a new fourth term, eq. (4), with a constant factor δ .

To verify the extended functional, turbulence simulations with artificially maintained sinusoidal zonal flow patterns of different k_r and shearing rates were used. Turbulence effects were removed by averaging over long time scales and large domains to obtain the deterministic stress response to the flow pattern. The resulting growth rate estimates are shown in figure 5. For a low shearing rate of $u = 0.1$ the growth rates for all modes are still positive. At a higher shearing rate of $u = 0.2$ the expected dip in the growth rate for low k_r occurs while a region of intermediate modes still grows. This corroborates the proposed behavior sketched in figure 4 and is in accordance with the observations in self-consistent simulations.

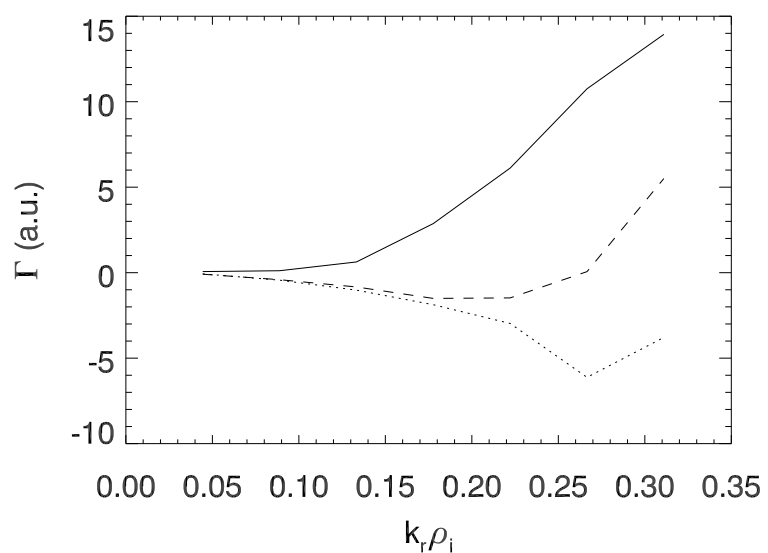


Figure 5: Growth rate dependence on k_r for different shearing rates; in arbitrary units $u = [0.1, 0.2, 0.25]$ for the continuous, dashed and dotted line respectively.

Conclusions

It was demonstrated that the Reynolds stress response functional (2), which already quantitatively reproduces the stress patterns of ITG-turbulence zonal flow simulations, requires an extension (5) to predict the time-evolution and characteristic intrinsic scale of the zonal flows. Artificial flows were used in turbulence computations to verify the damping at small k_r while an intermediate range of modes is still growing. Additional analysis of the high k_r behavior, the nonlinear interaction and dependence on the turbulence intensity gradient $\partial_r \ln I$ is required for a complete verification of the new response functional.

References

- [1] K. Hallatschek, A. Zeiler, *Physics of Plasmas* **7**, 2554 (2000)
- [2] K. Hallatschek, *Physical Review Letters* **93**, 6 (2004)
- [3] K. Itoh, K. Hallatschek, S. Toda, H. Sanuki, S. I. Itoh, *J. Phys. Soc. of Japan* **73**, 11, pp.2921-2923 (2004)